WILEY

Comparing the impacts of wildfire and meteorological variability on hydrological and erosion responses in a Mediterranean catchment

Jinfeng Wu[1,2] | Jantiene E. M. Baartman[2] | João Pedro Nunes[3]

[1]College of Land Science and Technology, China Agricultural University, Beijing, PR China

[2]Soil Physics and Land Management Group, Wageningen University and Research, Wageningen, The Netherlands

[3]CE3C–Centro de Ecologia, Evolução e Alterações Climáticas, Faculdade de Ciências, Universidade de Lisboa, Lisbon, Portugal

Correspondence
Jinfeng Wu, College of Land Science and Technology, China Agricultural University, Beijing 100193, PR China.
Email: jinfnegwu2020@163.com

Abstract

Land degradation and water resources pollution caused by catastrophic wildfires is of growing concern in fire-prone regions. Studies on the effects of wildfire on hydrology and erosion have mostly been conducted at plot or hillslope scale, while relatively few studies investigated post-wildfire hydrological responses and erosion at the meso-catchment scale ($\sim > 10$ km^2) in the Mediterranean. This study used measured discharge and suspended sediment at the outlet of a burnt catchment in southern Portugal, before and after a wildfire, to investigate post-wildfire changes in hydrological and erosion responses to rainfall. Hydrological and sediment connectivity patterns were derived to investigate changing dynamics induced by the fire within the catchment. The main findings were: (a) although a large part of the catchment experienced moderate to high severity burning, post-wildfire hydro-sedimentary response was considerably limited; (b) meteorological variability determined hydrological responses and erosion more strongly than wildfire effects; and (c) during the post-wildfire vegetation recovery period, only rainfall events with a high return period (~ 2 years) enhanced the hydrological and erosion responses. This can be explained by the spatial scale dependency of these processes and limited fine sediment supply, or relatively low connectivity in the study catchment. While connectivity is only an indicator, this implies that, at the meso-catchment scale, pollution of downstream water bodies by contaminated soil and ash may not occur immediately. Rather, because sediments and associated ashes and contaminants are first being transported to the areas around the stream networks, they only reach the outlet during heavy events which do connect the entire catchment. Thus, dynamic indices of connectivity that take rainfall event characteristics into consideration need to be further tested to assess and manage post-wildfire soil and water contamination risk.

KEYWORDS

hydrological responses, sediment connectivity, soil erosion, wildfire

1 | INTRODUCTION

Wildfire is a natural component of many ecosystems. However, in recent years, the increase in the frequency, size and severity of wild-fires is of growing concern in fire-prone regions around the world (Fill, Davis, & Crandall, 2019; Nunes et al., 2019; San-Miguel-Ayanz et al., 2012). As one of the most fire-prone regions in the world, European countries have experienced the worst fires in decades, such as two large fires in 2017 across central Portugal, a series of wildfires in 2018 in Greece and throughout much of Sweden, leading to loss of vegetation, property and life. With global warming, the severity and frequency of wildfires are projected to continue to increase, especially in the European Mediterranean and the latter region is experiencing some of the most significant impacts of global warming (Liu, Stanturf, & Goodrick, 2010; Turco et al., 2018).

Wildfires cause land degradation and downstream water pollution. Depending on the fire severity that represents the intensity of the fire or the released energy, wildfires can, partly or completely, consume surface litter and ground vegetation, and through heating and combustion processes alter physical, chemical and biological soil properties, for example, clogging of pores by ash, decreasing organic matter, increasing soil water repellency and changing soil aggregation (Mataix-Solera, Cerdà, Arcenegui, Jordán, & Zavala, 2011; Mataix-Solera, Gómez, Navarro-Pedreño, Guerrero, & Moral, 2002; Zavala, de Celis Silvia, & López, 2014). After a wildfire, quicker and enhanced hydro-sedimentary response to rainfall including more effective rainfall, quicker and higher runoff with more sediment delivery is observed in burnt areas, which is attributed to a decrease in ground interception, infiltration rates and shorter time to runoff, resulting in soil erosion and land degradation (Moody, Shakesby, Robichaud, Cannon, & Martin, 2013; Shakesby, 2011; Shakesby & Doerr, 2006). In addition, together with sediments, associated ashes and contaminants could be transported downstream, posing a risk to water resources (Campos et al., 2019; Robinne et al., 2018; Smith, Sheridan, Lane, Nyman, & Haydon, 2011).

However, as compared with pre-wildfire or non-burnt areas, post-wildfire hydrological and erosion response vary widely from muted to orders of magnitude higher, even extreme flooding and debris flow (Shakesby & Doerr, 2006). Differences in post-wildfire hydro-sedimentary response have been mainly attributed to the following factors. First, Ferreira, Coelho, Ritsema, Boulet, and Keizer (2008) and Stoof et al. (2012) stressed post-wildfire hydro-sedimentary response is largely affected by scale. Second, rainfall, topography, and soil properties have been accounted as dominant factors for post-wildfire hydro-sedimentary response at the catchment scale (Moody et al., 2013; Shakesby, 2011). Several studies reported a lack of increased post-wildfire hyro-sedimentary response because of the lack of rainfall, driving forces and available sediments (Estrany, López-Tarazón, & Smith, 2015; García-Comendador, Fortesa, Calsamiglia, Calvo-Cases, & Estrany, 2017; García-Comendador, Fortesa, Calsamiglia, Garcias, & Estrany, 2017; Moody & Martin, 2009; Owens, Blake, Giles, & Williams, 2012). Besides, burn severity is increasingly being recognised as a decisive factor controlling post-wildfire

hydrological responses and erosion rates (Benavides-Solorio & MacDonald, 2005; Larsen & MacDonald, 2007; Shakesby & Doerr, 2006; Vieira, Fernández, Vega, & Keizer, 2015); in this context, burn severity describes the degree to which a burnt area has been changed by a fire (Jain & Graham, 2007; Jain, Graham, & Pilliod, 2004; Keeley, 2009; UNOOSA, 2019). Consequently, quantitative empirical relations between burn severity and soil hydraulic properties (Moody et al., 2016), as well as between burn severity and soil erosion rates (Fernández & Vega, 2016b; Lanorte et al., 2019; Vieira et al., 2014) have been established in recent years.

This study investigated how hydrological and sediment connectivity modified by fire controls runoff and sediment delivery. Connectivity representing the linkage between system components stems from geomorphology and was applied in hydrology (Wohl et al., 2019). Hydrological and sediment connectivity can be divided into structural connectivity and functional connectivity, which are described as the degree of spatial linkage and the actual flux of water and sediment between system components, respectively (Heckmann et al., 2018). The index of connectivity (IC) proposed by Borselli, Cassi, and Torri (2008) is one of the most widely used indices of structural connectivity (Cavalli, Marchi, Goldin, Schenato, & Crema, 2015), which is calculated based on digital elevation model (DEM) and its' interaction with properties of the local land use and soil surface that affects sediment transport assigned as weighting factor. IC provides an estimate of the potential for sediment sources to reach specific targets areas. In this study, the IC was determined for both pre- and post-wildfire conditions and used as a spatial approach to understand the impacts of wildfire on hydrology and erosion processes.

Although the impacts of wildfire on hydrological and erosion responses have been extensively studied in fire-prone areas around the world at the plot or hillslope scale, only a few studies investigating post-wildfire hydrological and erosion responses at the meso-scale catchment scale ($\sim > 10$ km^2) exist, especially for the European Mediterranean area (Estrany et al., 2019; García-Comendador, Fortesa, Calsamiglia, Calvo-Cases, & Estrany, 2017; García-Comendador, Fortesa, Calsamiglia, Garcias, & Estrany, 2017; Inbar, Tamir, & Wittenberg, 1998; Mayor, Bautista, Llovet, & Bellot, 2007; Moody et al., 2013; Shakesby, 2011; Van Eck, Nunes, Vieira, Keesstra, & Keizer, 2016). This stems partly from wildfire contingency and destruction resulting in a scarcity of measurement data, but mostly from complex non-linear hydrological and erosion responses when scaling up (Moody et al., 2013). Studies at smaller catchment scale in the Mediterranean, typically draining an area of less than 1 km^2, observed that first-year runoff and sediment delivery following wildfire increased by more than 100-fold, and even 10,000-fold (García-Comendador, Fortesa, Calsamiglia, Calvo-Cases, & Estrany, 2017; Inbar et al., 1998; Mayor et al., 2007). However, due to the scale dependency of hydrological and erosion processes, the impacts of wildfire at larger catchment scale tends to be overestimated by plot- and hillslope-scale studies (Ferreira et al., 2008; Stoof et al., 2012). Consequently, accurate predictive assessments of fire-induced risk for water resources are hindered by the limited availability of databases on postfire hydrological and erosion effects at the larger scale (Robinne et al., 2018).

Given few catchment-scale studies and the importance of catchment dynamics for assessment of risks to soil and downstream water

resources, this study was conducted at the meso-catchment scale to investigate changes in hydrological and erosion responses to rainfall before and after wildfire, and the causes of any such changes. While this topic is of importance wherever wildfire occurs, it is of particular concern in the Mediterranean region due to wildfire frequency, limited water resources and already degraded soils. Hence the study site selected is in the Mediterranean's Iberian peninsula. Our main hypothesis follows the general conclusion of the reviewed literature, that significantly increased runoff and sediment delivery would be observed after wildfires, especially for catchments experiencing severe burning. To test this hypothesis and improve understanding of fire-induced hydrological changes and soil erosion at the scale of the catchment, runoff events were analysed for the Odeáxere catchment (18.53 km^2) in southern Portugal where a wildfire in early August 2003 burnt almost the entire catchment with moderate-to-high severity, and for which there was hydrological and sediment data available before and after the fire.

Multivariate statistical analysis was used to investigate hydrological and erosion responses to rainfall before and after the fire, and IC was calculated to detect the potential for the sediment to reach the outlet. The results can contribute to understanding the impacts of wildfire on hydrology and erosion processes at the meso-catchment scale, and related risks for soil and water resources.

2 | METHODS

2.1 | Study area

The Odeáxere catchment (18.53 km^2) is located in the south-western part of the Monchique Mountains in southern Portugal (Figure 1). Elevation ranges from 83 to 571 m above sea level (derived from the 10 m DEM of the Portuguese Geographic Institute - IGP), and decreases from north to south with a wide, relatively flat area around the catchment stream network. The whole catchment drains to the Bravura Reservoir, but multiple local irrigation ponds exist within the catchment, together comprising a drainage area of about 10% of the catchment (Figure 1). The region has a hot-summer Mediterranean climate (Csa in the Köppen-Geiger classification) (Kottek, Grieser, Beck, Rudolf, & Rubel, 2006) with average annual temperatures varying between 20 and 25°C. The average annual precipitation is 624 mm, with much more rainfall in winter than in summer. January is normally the coolest and the wettest month with an average of 98 mm rainfall, while July is the warmest and driest month with an average of 2 mm rainfall.

Land cover consists of Eucalypts and Mediterranean evergreen oaks in the upper parts of the catchment while shrubs and trees trimmed for fodder mainly occur in the lower parts (Figure 2a). Eight different soil types occur in the catchment but two types, that is,
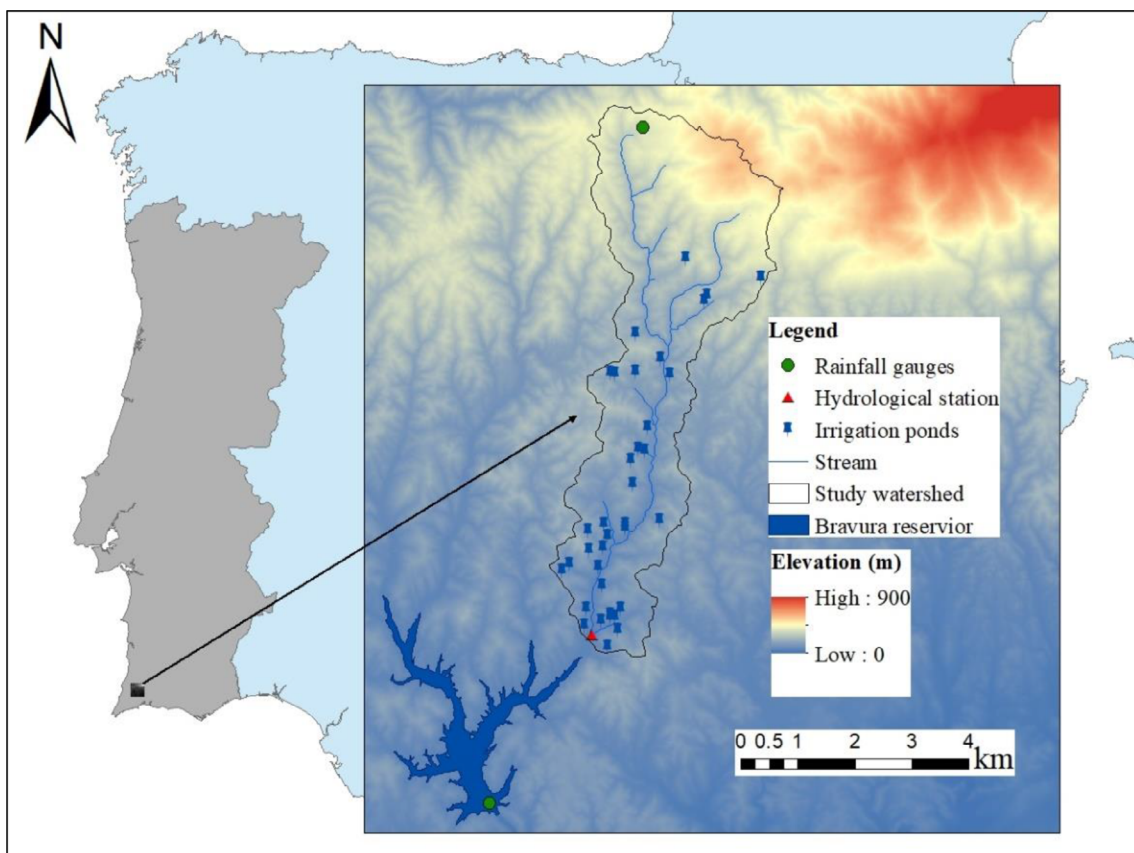

FIGURE 1 Study area, elevation and distribution of rainfall gauges, hydrological station, stream, irrigation ponds, and Bravura Reservoir [Colour figure can be viewed at wileyonlinelibrary.com]
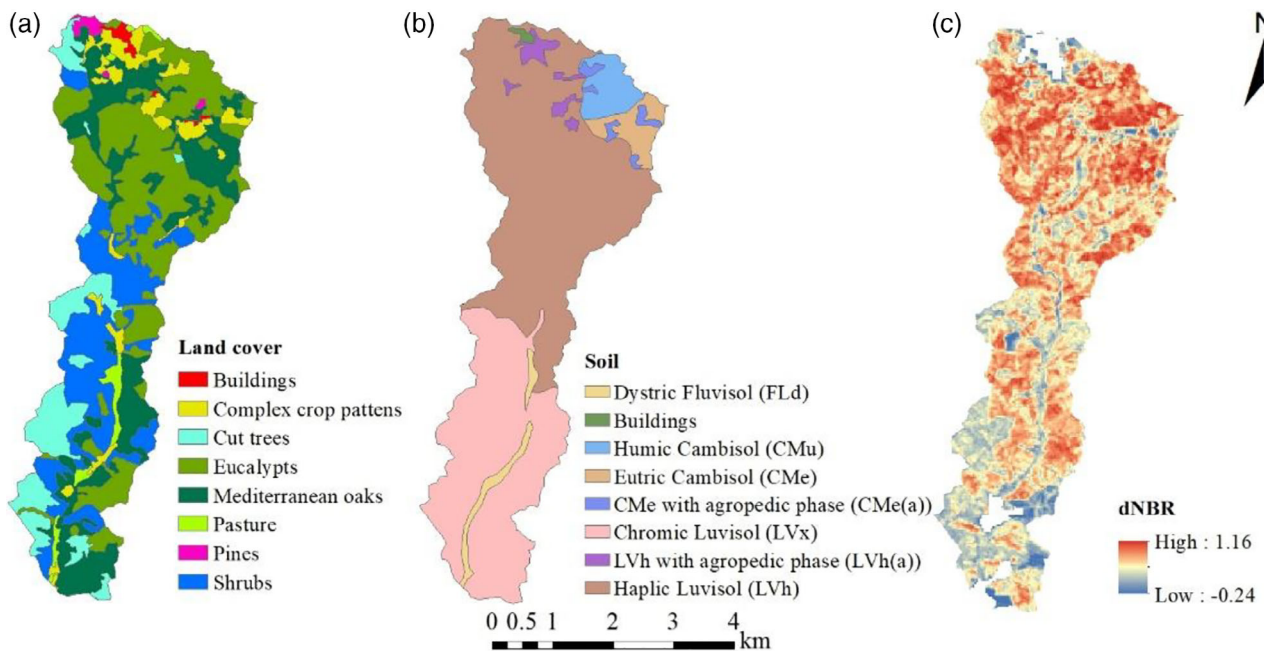
FIGURE 2 (a) Soil map; (b) Land cover map; (c) burn severity (dNBR) map of the Odeáxere study area [Colour figure can be viewed at wileyonlinelibrary.com]

Haplic and Chromic Luvisols (LVh and LVx), cover about 90% of the area (Figure 2b). Land cover was obtained from the 2007 1:25,000 land-use map from IGP and soil data was taken from the 1:25,000 soil map of the Portuguese Directorate-General for Agriculture and Rural Development - DGADR.

The Monchique region is prone to wildfires, and was burnt twice within the last two decades, in August 2003 and 2018 (ICNF, 2017). The wildfire in early August 2003 destroyed more than 21,300 ha. In this study, delta normalized burn ratio (dNBR) was used to reflect burn severity level (UNOOSA, 2019). The dNBR was calculated using the difference between the pre-fire and post-fire normalized burn ratio (NBR) obtained from LANDSAT-5 TM images of 30-m resolution (Figure 2c) (UNOOSA, 2019). As shown by the dNBR map, a very large amount of the surface area within the Odeáxere catchment was burnt with moderate-to-high severity (Figure 2c).

Following the fire, enhanced erosion has been recorded on several hillslopes of the region in a photographic inventory by local authorities (CMVB, 2005) and referred to in post-wildfire recovery plans for the Monchique Mountain Range (CNR, 2005). Few of these plans were implemented; in eucalypt forest plantations, most owners recovered burned logs and eucalypts were replanted or allowed to resprout, while there was little intervention in Mediterranean oaks and shrubland areas and vegetation was allowed to recover naturally. Plantation forest recovery was therefore faster than in remaining areas (Gouveia, DaCamara, & Trigo, 2010).

2.2 | Vegetation dynamics monitoring

The normalized difference vegetation index (NDVI) is a commonly used index to reflect vegetation dynamics from satellite imagery, but it has a strong seasonal oscillation. In order to eliminate NDVI's seasonal oscillation, DNDVI following Gouveia, Páscoa, and DaCamara (2018), was employed as the indicator to monitor vegetation dynamics for the analyzed period (2000–2010). NDVI values were retrieved from MOD13Q1 included in the MODIS Terra V6 product, which provides an adequate temporal and spatial resolution of, respectively, 250 m and 16 days (Didan, Munoz, Solano, & Huete, 2015). Subsequently, monthly NDVI time series were generated based on the pixel reliability index with good quality or marginal quality.

2.3 | Rainfall and outlet measurements and analysis

Hourly data for rainfall, streamflow, conductivity and turbidity between October 2001 and September 2006 were obtained from the Portuguese Environment Agency through the National Water Resource Information System (SNIRH, 2019). Hourly rainfall was measured in two rainfall gauges located in the north and south of the Odeáxere catchment (Figure 1). Hourly water level was measured at the stream outlet and streamflow discharge was calculated with a stage-discharge curve also provided by SNIRH (Figure 1). At the same location, hourly water conductivity and turbidity were measured with an automatic sensor; suspended sediments were calculated from turbidity using a linear relationship (sediments = 2.1 x turbidity, $r^2 > 0.99$), built from monthly water samples taken from the same site and analysed for suspended sediment concentration, including during a period of high streamflow and turbidity; this data was also taken from SNIRH. Turbidity data was limited to values under 999 NTUs

due to sensor saturation, which led to an underestimation of suspended sediments during peak sediment flow periods of some storms. The hydrometric data series started in August 2001 and is still being updated; the turbidity data series started in December 2001, presented significant gaps in 2005, with measurement stopping in 2006.

The intensity-duration-frequency (IDF) curve is a mathematical function that relates rainfall intensity with its duration and the return period. The regional IDF curves were constructed for the Monchique rainfall gauge (Brandão, Rodrigues, & Costa, 2001), and were used in this study to estimate the return period of selected pre-wildfire and post-wildfire rainfall-runoff events.

2.4 | Runoff events

Given two rainfall gauges located at the top and bottom of this catchment, hourly rainfall from the two rainfall gauges was averaged to calculate the rainfall characteristics of the analysed events. Maximum rainfall intensity in 30 min for each event was estimated based on relationships with maximum hourly rainfall (Brandão et al., 2001). All runoff events with total rainfall greater than 9 mm and available turbidity data were selected to be analysed. Based on the hydrograph of each event, streamflow discharge was separated into surface runoff and baseflow using an automated filter technique (Arnold, Allen, Muttiah, & Bernhardt, 1995).

Events were considered to begin with the first rainfall, and end when surface runoff was over, except when a new rainfall event started before discharge of the previous one was finished, in which case the first event was considered to end when the second one began. A total of 39 events were selected between October 2001 and September 2006, and are listed E1-E39 in chronological order of occurrence (Table 1; Figure 4d); there was a limited selection of events in years 4 and 5 due to the severe 2004/05 drought and the subsequent data gaps in the turbidimeter. Although the wildfire occurred in July 2003, a hydrological year was used since it encompasses a full wet/dry seasonal cycle. In this region, a hydrological year is defined as the timespan between October 1 and September 30 of the next year. The study period was therefore divided into 5 hydrological years.

TABLE 1 Hydrological years and runoff events

Hydrological years	Runoff events No.
Yr 1:2001 / 2002	E1 - E13 (E2, E8, and E9 with peak turbidity >999NTUs)
Yr 2:2002 / 2003	E14 - E27 (E18, E20, and E21 with peak turbidity >999NTUs)
Yr 3:2003 / 2004	E28 - E36 (E28 and E32 with peak turbidity >999NTUs)
Yr 4:2004 / 2005	E37
Yr 5:2005 / 2006	E38 - E39 (E38 and E39 with peak turbidity >999NTUs)

2.5 | Statistical analysis

For each runoff event, the following meteorological variables were determined (Table 2): rainfall duration (P_{dura}, h); rainfall amount (P, mm); rainfall intensity (IP, mm h^{-1}); maximum rainfall intensity in 30 min ($IP30_{max}$, mm h^{-1}); and relative time-to-maximum rainfall intensity ($IPRT_{max}$). $IPRT_{max}$ was calculated using time to maximum rainfall intensity divided by rainfall duration. $IP30_{max}$ was calculated from maximum hourly rainfall, using existing relationships between hourly and 30 mins rainfall (Brandão et al., 2001).

The antecedent precipitation index (API) and initial baseflow (Q_i, m^3 s^{-1}) were also included to describe antecedent conditions prior to each runoff event. API was calculated using the equation proposed by Kohler and Linsley (1951) and based on the rainfall of the previous 10 days.

In addition, the following hydrological variables were determined for each event (Table 2): runoff duration (R_{dura}, h); runoff (R, mm); runoff coefficient (RC); total discharge (Q, m^3 s^{-1}); base discharge fraction (Q_b, %); peak discharge (Q_{peak}, m^3 s^{-1}); and relative time-to-peak discharge (QRT_{peak}). QRT_{peak} was calculated from time to peak discharge divided by runoff duration. The transport of sediment by discharge was characterized by suspended sediment (SS, g l^{-1}) and sediment yields (SY, kg). SY is not represented in this study because peak SS was missing and SY was well related to R and Q (Pearson's correlation coefficient, $p < 0.05$).

Fire impacts (DNDVI and dNBR) were not added, as a preliminary analysis (not shown) did not reveal relationships with hydrological and sediment response; the classification of events as pre-fire or post-fire

TABLE 2 Variables used to characterize the rainfall-runoff events

	Variables	Description (units)
Meteorological variables	P_{dura}	Rainfall duration (h)
	P	Rainfall amount (mm)
	IP	Rainfall intensity (mm h^{-1})
	$IP30_{max}$	Maximum rainfall intensity in 30 min (mm h^{-1})
	$IPRT_{max}$	Relative time-to-maximum rainfall intensity (h)
Antecedent conditions	API	The antecedent precipitation index (–)
	Q_i	Initial baseflow discharge (m^3 s^{-1})
Hydro-sediment variables	R_{dura}	Runoff duration (h)
	R	Runoff (mm)
	RC	Runoff coefficient (–)
	Q	Total discharge (m^3 s^{-1})
	Q_b	Baseflow discharge fraction (%)
	Q_{peak}	Peak discharge (m^3 s^{-1})
	QRT_{peak}	Relative time-to-peak discharge (h)
	SSC	Suspended sediment concentration (g l^{-1})

was considered sufficient, with DNDVI indicating the occurrence of a post-fire vegetation disturbance.

Boxplots were used to summarize and display the distribution of variables based on a five-number summary (first quartile (Q1), median, third quartile (Q3), 'minimum' or Q1-1.5* interquartile range (IQR), and 'maximum' or Q3 + 1.5*IQR) and mean. The Wilcoxon–Mann–Whitney test was used to analyse the occurrence of significant differences between runoff events. Principal components analysis (PCA) was used to explore the relationships between all variables for individual events. All statistical analyses were conducted using the R statistical package (Core Team Development, 2018).

2.6 | Index of connectivity

In this study, the Index of Connectivity (IC; Borselli et al., 2008) was estimated using the stand-alone freely available software SedInConnect 2.3 (Crema & Cavalli, 2018). The calculation includes an estimation of the upslope contributing area and the downslope pathway to a pre-defined target (here: the catchment outlet). Details on the calculation can be found in Borselli et al. (2008), Cavalli et al. (2015), and Crema and Cavalli (2018). The 10 m DEM described earlier and a weighting factor are primarily required as input data. As in many studies (Borselli et al., 2008; Fernández, Fernández-Alonso, & Vega, 2020; Foerster, Wilczok, Brosinsky, & Segl, 2014; Martínez-Murillo & López-Vicente, 2018), the RUSLE C-factor was used as weighting factor. Two IC maps were calculated; one for the pre-wildfire and one for the post-wildfire situation, thus requiring C-factor values for unburnt land uses as well as for burnt conditions. The pre-wildfire weighting factor map was derived from the RUSLE C-factor based on the COS2007 land cover map (Table 3) (Carvalho-Santos, Nunes, Monteiro, Hein, & Honrado, 2016; Nunes et al., 2018) while the post-wildfire weighting factor map was calculated based on the burn severity map using the RUSLE C-factor estimated for different severity classes by multiple authors (Table 4) (Fernández & Vega, 2016a; Larsen & MacDonald, 2007; Vieira et al., 2014), which were calibrated by the authors.

3 | RESULTS

3.1 | Variation in vegetation

Vegetation dynamics, estimated by the DNDVI values from 2001 to 2010, are shown in Figure 3. In pre-wildfire years (January 2001 to June 2003), DNDVI fluctuated between 0.84 and 1.05 with a slight seasonal pattern. After the wildfire, the DNDVI value dropped dramatically to 0.36. Within the half year following the wildfire, the DNDVI quickly recovered to 0.74, and then fluctuated strongly between 0.57 and 1.01 during the 7 years after the wildfire, with a slightly more pronounced seasonal pattern.

3.2 | Daily rainfall, discharge and suspended sediment

Daily rainfall, discharge and suspended sediment are shown in Figure 4 for the 5-hydrological year period from October 2001 to September 2006. Rainfall was much lower during the first two hydrological years after the fire (591 mm in 2003/2004 and 354 mm in 2004/2005, respectively), compared to the other years (815 mm in 2001/2002, 799 mm in 2002/2003, and 836 mm in 2005/2006). Accordingly, relatively lower discharge and suspended sediment concentration were measured at the outlet during the first two hydrological years after the fire, especially in 2004/2005 which was the driest (Figure 4b,c). Despite this, it also can be noticed that wildfire contributed to increasing hydro-sedimentary response, for example, the largest daily discharge amount during the study period was recorded in 2003/2004, the year immediately following the fire.

Additionally, rainfall had a strongly seasonal pattern typical of Mediteranean climates. Less than 6% of the total annual rainfall was recorded during summer while more than 41% was recorded during winter. Therefore, more discharge with more suspended sediment was recorded from November to April, mostly during the wet season during which more than 68% of the total annual rainfall occured.

3.3 | Rainfall characteristic of pre- and post-wildfire runoff events

Runoff events were not equally distributed among the hydrological years from October 2001 to September 2006, or between the years before and after the fire (Figure 4d). There were 27 runoff events recorded in the pre-wildfire period (October 2001 to June 2003; almost 1.5 hydrological years), while only 12 events were recorded in the post-wildfire period (August 2003 to August 2006, almost 3 hydrological years). Despite the difference in number of events, there were no statistically significant differences for the meteorological variables

TABLE 4 USLE C factor for burn severity

dNBR	<0.1	0.1–0.44	0.44–0.66	>0.66
USLE C factor	0.001	0.005	0.020	0.100

TABLE 3 USLE C factor for land cover

Land use	Buildings	Complex crop pattern	Pasture	Mediterranean oaks	Eucalypts	Pines	Shrubs	Cut trees
USLE C factor	0.001	0.005	0.001	0.001	0.001	0.001	0.002	0.002

FIGURE 3 Variation in DNDVI from 2001 to 2010; the vertical dotted line indicates the date of wildfire occurrence [Colour figure can be viewed at wileyonlinelibrary.com]
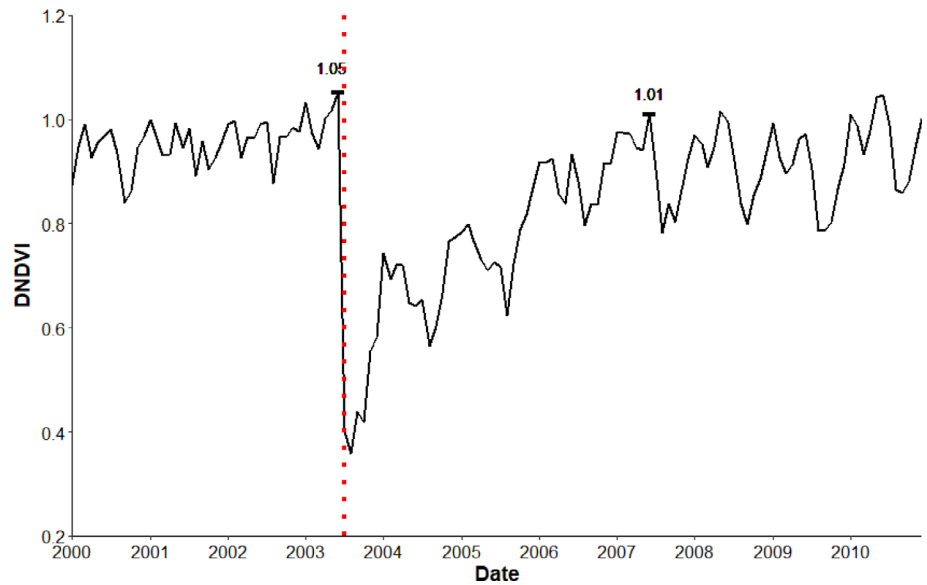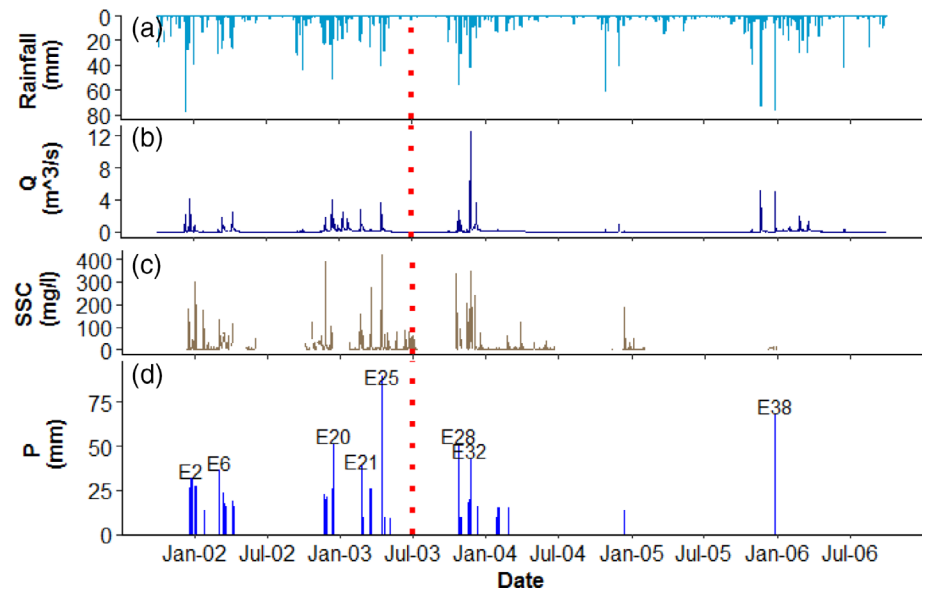

FIGURE 4 (a) Daily Rainfall (mm); (b) Daily discharge (m^3 s^{-1}); (c) Daily suspended sediment (mg/l); (d) Selected runoff event numbers, with the major events marked; the vertical dotted line across all figures indicates the date of wildfire occurrence [Colour figure can be viewed at wileyonlinelibrary.com]

between pre- and post-wildfire events (Wilcoxon, $p < 0.05$) (Figure 5). This indicates that although the number of runoff events was different, their characteristics were comparable.

According to the distribution of individual rainfall events on the Monchique's IDF curve (Figure 6), most of the events were medium and low-intensity events with return periods of less than 1 year in the Monchique region. Exceptions to this were two events with return periods around 2 years: pre-wildfire event E25, which had the longest duration; and post-wildfire event E38, which had the highest intensity.

3.4 | Hydro-sedimentary response

The hydrologic variables API, Q_i, and Q_b were similar for pre-wildfire and post-wildfire events (Figure 5), with no statistically significant differences ($p < 0.05$). Unexpectedly, there was also no statistically significant difference for any of the hydro-sedimentary variables. Nevertheless, post-wildfire events had, on average, shorter runoff duration and relatively shorter time-to-peak discharge; both can be at least partially explained by a shorter rainfall duration, although the differences were more marked for runoff (lower p values). It should especially be noted that relative time-to-peak runoff (QRT_{peak}) after the wildfire was lower than before the fire, despite similar values for time-to-peak rainfall ($IPRT_{max}$), indicating a change in runoff response caused by different catchment conditions. Also, post-wildfire events showed higher runoff, discharge, peak discharge and sediment concentration, despite similar rainfall amount, rainfall intensity and antecedent precipitation values. The RC was also higher for post-wildfire events compared to pre-wildfire events, even though both were low.
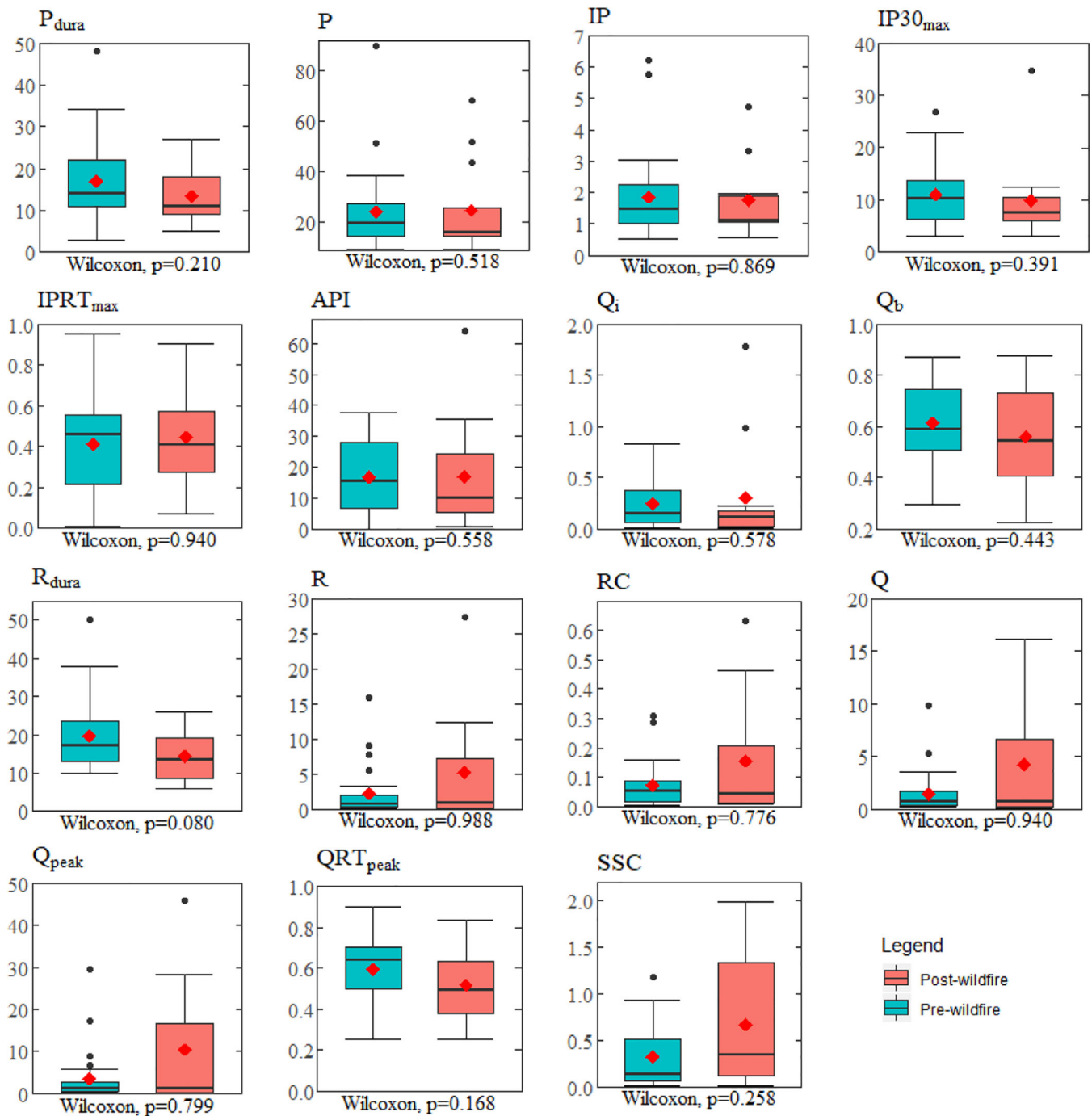
FIGURE 5 Boxplots of rainfall, antecedent conditions and hydro-sedimentary variables (See Table 2) for pre-wildfire (Left) and post-wildfire (Right) events. Boxes show first quartile (Q1), median, third quartile (Q3), interquartile range (IQR), Q1-1.5*IQR, and Q3 + 1.5*IQR, as well as outliers (dark circles), mean (red diamond) and Wilcoxon–Mann–Whitney test significance value [Colour figure can be viewed at wileyonlinelibrary.com]

Besides, PCA was performed; Q_b, R_{dura}, R, RC, Q, Q_{peak}, QRT_{peak} and SSC from hydro-sedimentary variables were used as experimental variables, and DNDVI, rainfall variables and antecedent conditions were consequently used as supplementary variables.

The results of the PCA are presented in Figure 7. In combination, the first two axes of the PCA analysis accounted for 79.83% of the total variances with axis 1 at 64.10% and axis 2 at 15.73%. The amount of hydrological and sediment responses (Q_b, R, RC, Q, Q_{peak} and SSC) loaded highly onto axis 1 while runoff duration loaded highly onto axis 2. Among the supplementary variables, P, IP and $IP30_{max}$ were well correlated with axis 1, while P_{dura} was well correlated with axis 2. In contrast, DNDVI was not closely related to the hydro-sedimentary variables. Besides, $IPRT_{max}$, API and Q_i did not correlate well with the hydro-sedimentary variables.
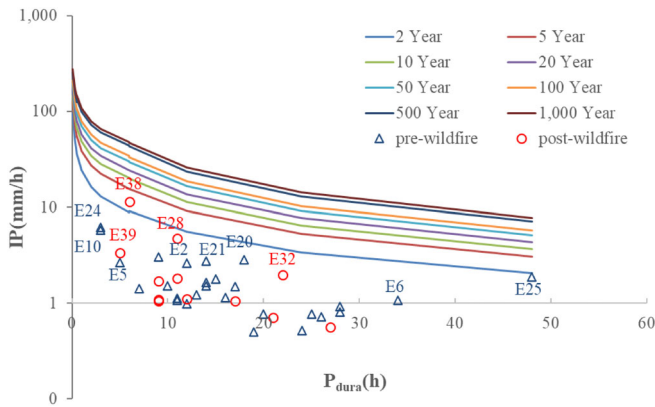
FIGURE 6 Monchique's IDF curves of varying return periods with the precipitation events selected and analyzed in this study (blue triangles are pre-wildfire events, red circles are post-wildfire events) [Colour figure can be viewed at wileyonlinelibrary.com]

This indicates that rainfall-related variables (P_{dura}, P, IP and $IP30_{max}$) were more important for hydrological and erosion responses in this catchment when compared with the wildfire impacts on vegetation and soil.

Consequently, the distribution of individual events does not show the differences between pre- and post-wildfire on the PCA plane; most of individual events with return periods below 1 year (small events) are located on the left of the PCA plane, which led to low hydrological and erosion responses in both periods, whereas few storms with long return periods (big events) are located on the right
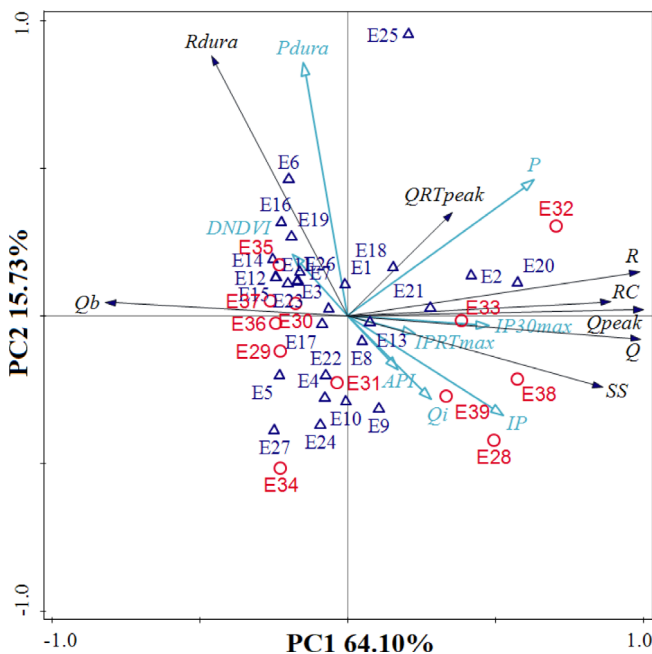
lower quadrant of the PCA plane, which led to quicker and higher run-off generation with more suspended sediment after the fire compared with before the fire. Only these big events shows some differences between pre- and post-wildfire. As shown in Figure 7, for big events, the pre-wildfire events E2, E8, E9, E13, E18, E20, E21 and E25 are situated to the upper left side of the post-wildfire events E28, E32, E33, E38 and E39, which indicates wildfire did increase hydrological and erosion responses.

3.5 | Index of connectivity

Figure 8 shows boxplots of the IC values for before and after the fire. As expected, post-wildfire IC values, on average, increased by 20% compared to pre-wildfire values. Despite this, IC in this catchment was quite low for both conditions (average of −10.4 and − 8.4 for pre-wildfire and post-wildfire, respectively, Figure 8).

The spatially explicit IC before and after the fire is shown in Figure 9, revealing clearly different patterns for pre- and post-wildfire conditions. Before the fire, the relatively higher IC values occurred close to the channels and outlet, whereas, after the fire, the higher values were distributed throughout the entire catchment. In addition, the differential IC map (Figure 9c; post-wildfire IC minus pre-wildfire IC) shows that, after the fire, IC values that had increased by more than 2.5 were located in the upper parts of the catchment, while IC values increased by less than 1.5 were in the lower parts of the catchment close to the outlet. Thus, even though IC was higher post-wildfire than pre-wildfire, the largest
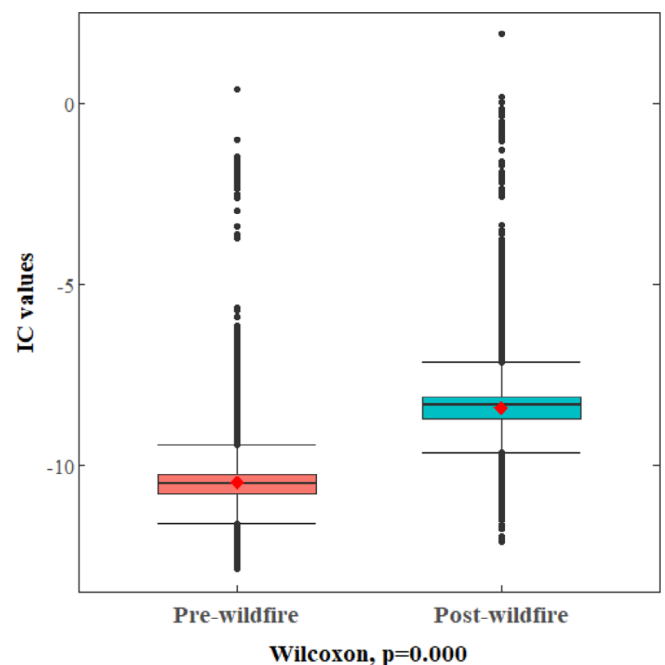

FIGURE 7 The plane of PCA analysis (blue triangles are pre-wildfire events, red circles are post-wildfire events) [Colour figure can be viewed at wileyonlinelibrary.com]

FIGURE 8 Boxplot of sediment connectivity (IC values) before and after the fire for the study catchment [Colour figure can be viewed at wileyonlinelibrary.com]
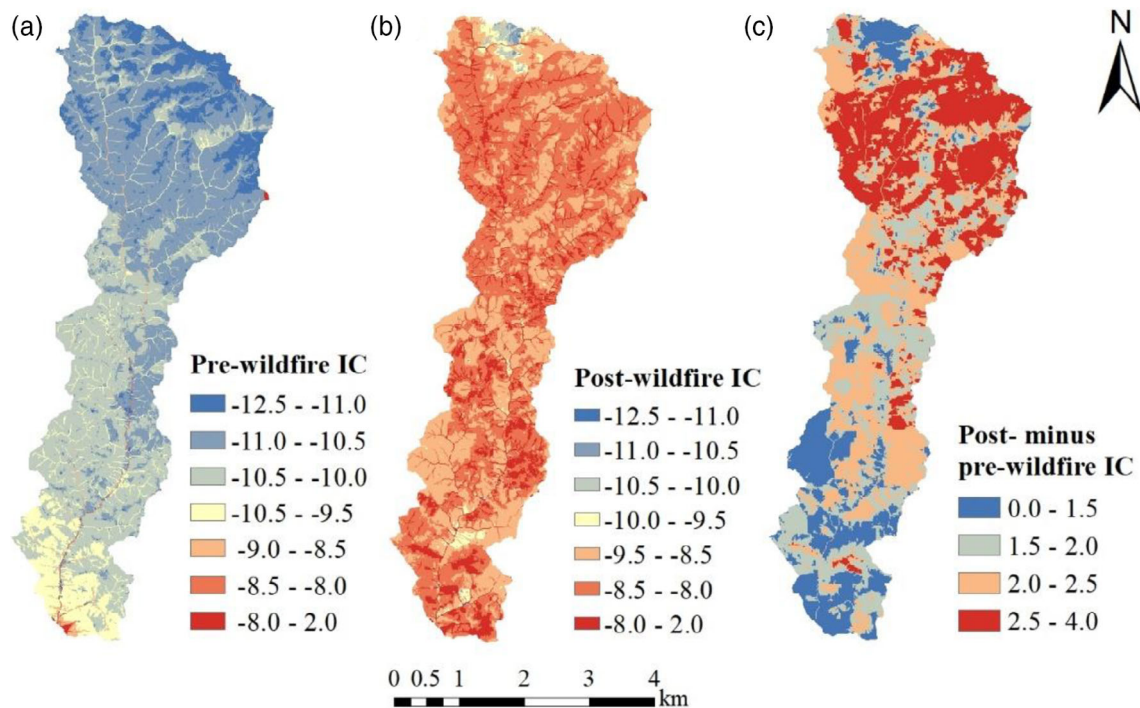
FIGURE 9 Map of the connectivity index (IC) (a) before the fire, (b) after the fire and (c) difference between pre- and post-wildfire [Colour figure can be viewed at wileyonlinelibrary.com]

increases occurred at relatively large distances from the catchment outlet.

4 | DISCUSSION

Although the vegetation index showed a remarkable recovery within the half year following the wildfire, the window of disturbance lasted a longer period of 3–7 years in this catchment. These results are consistent with the findings of Gouveia et al. (2018) that a broadleaved forest dominated by eucalypts that has recovered to near pre-wildfire conditions would require between 3 and 6 years, although ground cover recovered quickly. Unfortunately, only few correct measurement data (discharge and turbidity) spanning the post-wildfire 2.5 years remained for the analysis and most of the selected runoff events occurred within the first post-wildfire year. During the recovery period of post-wildfire vegetation, increased hydrological and erosion responses were observed in the study area, in which similar rainfall and antecedent conditions did lead to, on average, quicker hydrological response as well as about a two-fold increase in runoff and suspended sediment after the fire compared to before the fire. However, compared with other Mediterranean studies at the catchment scale (García-Comendador, Fortesa, Calsamiglia, Calvo-Cases, & Estrany, 2017; Inbar et al., 1998; Mayor et al., 2007), post-wildfire hydro-sedimentary response was considerably limited in this study. For example, even conducting in a terraced Mediterranean catchment (4.8 km²) with limited post-wildfire the hydrosedimentary response, García-Comendador, Fortesa, Calsamiglia, Calvo-Cases, and

Estrany (2017) reported that suspended sediment were more than 100-fold higher than that in the non-burnt terraced catchment. As our study catchment is relatively large (18.53 km²), the observed, considerably limited post-wildfire hydro-sedimentary response, is probably mainly caused by the scale dependency of hydrological and erosion processes, which is in agreement with Ferreira et al. (2008) and Stoof et al. (2012). Indeed, enhanced erosion on the fire-affected hillslopes of the southern Monchique mountains was recorded in a photographic inventory (CMVB, 2005) and referred to in post-wildfire recovery plans (CNR, 2005), although hillslope erosion data was not collected after the 2003 wildfire. Probably, limited hillslope sediments were transported to the stream channel system, which was also found by Estrany et al. (2015) and García-Comendador, Fortesa, Calsamiglia, Garcias, and Estrany (2017) who used fallout radionuclide tracers to understand the impacts of wildfire on sediment delivery in a Mediterranean catchment. In addition, both studies suggest that wildfires can significantly enhance sediment delivery when linked with sufficient rainfall (Estrany et al., 2015; García-Comendador, Fortesa, Calsamiglia, Garcias, & Estrany, 2017), consistent with the result of our study. That is also the main reason why low impacts of wildfire on hydro-sedimentary response occurred in other burnt catchments (Moody & Martin, 2009; Owens et al., 2012; Prosser & Williams, 1998).

Besides, considerably limited post-wildfire hydro-sedimentary response is partially caused by a thin soil layer with a large volume of stones in this study area. About 90% of the study area comprises soils developed from schists or greywackes, which have a stone content of 39% (LVh) and 46% (LVx, see Figure 2a) on the topsoil layer, respectively. As Cerdan et al. (2010) and Shakesby (2011) discussed, stones

can increase infiltration by increased surface roughness, affect soil water repellency, and protect fine sediment from being transported, resulting in supply-limited conditions for erosion. By contrast, studies from the USA and Australia, also at the catchment scale, did find enhanced erosive response after wildfire (Cannon, Gartner, Wilson, Bowers, & Laber, 2008; Jackson & Roering, 2009; Nyman, Sheridan, Smith, & Lane, 2011). However, in those areas, mostly flooding and debris flows occurred, which mainly depend on short duration, high intensity storms as drivers and the availability of fine sediment supply (Cannon et al., 2008; Smith et al., 2012), which generate sufficient transport capacity of flows (Smith et al., 2011). Again, post-wildfire hydro-sedimentary responses at the catchment scale largely depend on physical and anthropogenic environmental characteristics (García-Comendador, Fortesa, Calsamiglia, Calvo-Cases, & Estrany, 2017; Shakesby, 2011).

Notably, irrigation ponds in this region were not a cause of the low hydrological and erosion responses. Although the study area contains 36 ponds which, combined, account for about 10% of the drainage area of this catchment, most of them are located in the lower part of the catchment with low burn severity (Figure 1). Keizer et al. (2015) reported low sediment yields can be explained by irrigation ponds because some of sediments were retained in ponds. However, in our case, the effect of irrigation ponds does not extend to the entire catchment. So we would refer to this as another scale issue, where the effects of irrigation ponds on smaller-scale sediment transport cannot be upscaled directly.

Finally, and arguably most importantly, as expected, limited post-wildfire hydro-sedimentary response can be explained by connectivity. In our study area, both pre- and post-wildfire ICs were quite low. Even though post-wildfire IC in our catchment increased by 20%, the fire-increased connectivity was mainly located in the upstream part of the catchment, at relatively large distances from the catchment outlet (Figure 9c). As a result, increased overland flow that did occur post wildfire were likely absorbed in the more highly connected upper parts of the catchment and therefore did not reach the lower parts and outlets. These results suggest that IC can be a useful spatial analysis tool for assessing changes in hydrological and erosion processes, especially caused by land abandonment and wildfire. To date, changes in hydrological and sediment connectivity have not often been studied in relation to wildfire. Some studies linked connectivity to exploring post-wildfire hydrological and erosion responses or soil degradation (Calsamiglia et al., 2018; Calsamiglia, Lucas-Borja, Fortesa, García-Comendador, & Estrany, 2017; Estrany et al., 2019; Fernández et al., 2020; Martínez-Murillo & López-Vicente, 2018). These studies were conducted at a smaller scale (< 5km^2), which makes the results difficult to compare to our study at larger-scale catchment. However, they support the conclusion that connectivity can be a promising approach for assessing changes in hydrological and erosion processes.

Taken together, our findings suggest that, at least in the region studied, instead of wildfires posing immediate risk of downstream aquatic contamination (Campos et al., 2019; Carvalho et al., 2019), factors such as the scale dependency of hydrological and erosion processes within a catchment, supply-limited fine soil and low connectivity, can impact that risk and result in little effect of wildfire on downstream water resources. None the less, as a result of significantly enhanced soil erosion on the sub-catchment hillslopes, sediments could remain in the relatively flat areas around the stream networks, causing associated ash and other contaminants to form a longer-term (slower) risk for downstream water contamination.

Further, if an extreme storm event occurs during post-wildfire vegetation recovery, significantly enhanced hydrological and erosion responses would be expected, as suggested by the comparison between low and high return period events shown earlier, with associated increases in risk to downstream waters. Hence, it would be interesting to test more dynamic indices of connectivity which consider functional connectivity dependent on rainfall event characteristics. Alternatively, numerical modelling could help explore, in greater detail, the differences between pre-wildfire and post-wildfire small and large rainfall events in a spatially-distributed way.

5 | CONCLUSIONS

We analyzed the hydrological and erosion responses to a wildfire at the meso-catchment scale ($\sim$ > 10 km^2), for a Mediterranean catchment, using a combination of assessment of sediment connectivity before and after wildfire and PCA analysis of runoff events. This study showed that post-wildfire events had, on average, faster and higher runoff responses with a two-fold increase in suspended sediment as compared to pre-wildfire events. However, post-wildfire hydro-sedimentary response were considerably limited. We also found that wildfire itself was less important for hydrological and sediment responses than meteorological variability. We conclude that, for the conditions of the region studied, wildfire-enhanced overland flow and sediment transport does occur locally on hillslopes with high burn severity, however the enhanced flow and transport will not necessarily reach the outlet of the catchment due to the scale dependency of hydrological and erosion processes and supply-limited fine soil conditions or low connectivity. Our results support the hypothesis that wildfire can enhance hydrological and sediment responses; however, the impacts of wildfire on soil and downstream water risk contamination may be overestimated when upscaling plot- or hillslope-scale studies to the catchment-scale.

That said, enhanced soil erosion on sub-catchment hillslopes during post-wildfire vegetation recovery may lead to increased chance of longer-term (slower) downstream water risk contamination, and extreme events during the same period could significantly enhance hydrological and erosion responses with more rapid downstream impact. Therefore, we suggest that testing of more dynamic indices of connectivity which consider functional connectivity dependent on rainfall event characteristics is needed. Alternatively, modelling could be used to investigate more detailed differences between the impacts of small and large pre-wildfire and post-wildfire rainfall events. Increased recognition and consideration of multiple dynamics with catchments, for example, connectivity, can contribute to increased

understanding of the likely impacts of wildfires and probable management needs.

DATA AVAILABILITY STATEMENT

The data that support the findings of this study are openly available in the Portuguese Water Resources Information System (SNIRH) at https://snirh.apambiente.pt/.

ORCID

Jinfeng Wu https://orcid.org/0000-0002-2875-8628
João Pedro Nunes https://orcid.org/0000-0002-0164-249X

REFERENCES

Arnold, J., Allen, P., Muttiah, R., & Bernhardt, G. (1995). Automated Base flow separation and recession analysis techniques. *Groundwater*, 33(6), 1010–1018. https://doi.org/10.1111/j.1745-6584.1995.tb00046.x

Benavides-Solorio, J. d. D., & MacDonald, L. H. (2005). Measurement and prediction of post-fire erosion at the hillslope scale, Colorado Front Range. *International Journal of Wildland Fire*, 14(4), 457–474. https://doi.org/10.1071/WF05042

Borselli, L., Cassi, P., & Torri, D. (2008). Prolegomena to sediment and flow connectivity in the landscape: A GIS and field numerical assessment. *Catena*, 75(3), 268–277. https://doi.org/10.1016/j.catena.2008.07.006

Brandão, C., Rodrigues, R., & Costa, J. P. (2001). Análise De Fenómenos Extremos. Precipitações Intensas em Portugal Continental. *Direcção dos Serviços de Recursos Hídricos*.

Calsamiglia, A., Fortesa, J., García-Comendador, J., Lucas-Borja, M. E., Calvo-Cases, A., & Estrany, J. (2018). Spatial patterns of sediment connectivity in terraced lands: Anthropogenic controls of catchment sensitivity. *Land Degradation & Development*, 29(4), 1198–1210. https://doi.org/10.1002/ldr.2840

Calsamiglia, A., Lucas-Borja, M. E., Fortesa, J., García-Comendador, J., & Estrany, J. (2017). Changes in soil quality and hydrological connectivity caused by the abandonment of terraces in a Mediterranean burned catchment. *Forests*, 8(9), 1–20. https://doi.org/10.3390/f8090333

Campos, I., Abrantes, N., Pereira, P., Micaelo, A. C., Vale, C., & Keizer, J. J. (2019). Forest fires as potential triggers for production and mobilization of polycyclic aromatic hydrocarbons to the terrestrial ecosystem. *Land Degradation & Development*, 30(18), 2360–2370. https://doi.org/10.1002/ldr.3427

Cannon, S. H., Gartner, J. E., Wilson, R. C., Bowers, J. C., & Laber, J. L. (2008). Storm rainfall conditions for floods and debris flows from recently burned areas in Southwestern Colorado and Southern California. *Geomorphology*, 96(3–4), 250–269. https://doi.org/10.1016/j.geomorph.2007.03.019

Carvalho, F., Pradhan, A., Abrantes, N., Campos, I., Keizer, J. J., Cassio, F., & Pascoal, C. (2019). Wildfire impacts on freshwater detrital food webs depend on runoff load, exposure time and burnt forest type. *Science of the Total Environment*, 692, 691–700. https://doi.org/10.1016/j.scitotenv.2019.07.265

Carvalho-Santos, C., Nunes, J. P., Monteiro, A. T., Hein, L., & Honrado, J. P. (2016). Assessing the effects of land cover and future climate conditions on the provision of hydrological services in a medium-sized watershed of Portugal. *Hydrological Processes*, 30(5), 720–738. https://doi.org/10.1002/hyp.10621

Cavalli, M., Marchi, L., Goldin, B., Schenato, L., & Crema, S. (2015). Toward the development of a stand-alone application for the assessment of sediment connectivity. *Rendiconti Online Della Società Geologica Italiana*, 34, 58–61. https://doi.org/10.3301/rol.2015.37

Cerdan, O., Govers, G., Le Bissonnais, Y., Van Oost, K., Poesen, J., Saby, N., … Dostal, T. (2010). Rates and spatial variations of soil erosion in Europe: A study based on erosion plot data. *Geomorphology*, 122(1–2), 167–177. https://doi.org/10.1016/j.geomorph.2010.06.011

CMVB (2005). *Recuperação Hidrológico-Florestal Do Perímetro Florestal De Vila Do Bispo E Área Envolvente*. Vila Do Bispo: Câmara Municipal De Vila Do Bispo (Cmvb). https://cms.cm-viladobispo.pt/upload_files/client_id_1/website_id_1/Servicos/Protecao%20Civil/Planeamento/plano%20recupera%C3%A7%C3%A3o%20hidrologico-florestal%20perimetro%20florestal%20vb%20.pdf

CNR (2005). *Orientações Estratégicas Para a Recuperação Das Áreas Ardidas Em 2003 E 2004*, Lisboa: Retrieved from http://www2.icnf.pt/portal/florestas/dfci/relat/raa/resource/doc/CNR-OER-Docfinal.pdf

Core Team Development, R. (2018). *R: A language and environment for statistical computing (version 3.5.0)*. Retrieved from https://www.r-project.org/.

Crema, S., & Cavalli, M. (2018). Sedinconnect: A stand-alone, free and open source tool for the assessment of sediment connectivity. *Computers & Geosciences*, 111, 39–45. https://doi.org/10.1016/j.cageo.2017.10.009

Didan, K., Munoz, A. B., Solano, R., & Huete, A. (2015). *Modis vegetation index user's guide (Mod13 series)*. Vegetation Index and Phenology Lab, Tucson, AZ: The University of Arizona, 1–38.

Estrany, J., López-Tarazón, J. A., & Smith, H. G. (2015). Wildfire effects on suspended sediment delivery quantified using fallout radionuclide tracers in a Mediterranean catchment. *Land Degradation & Development*, 27(5), 1501–1512. https://doi.org/10.1002/ldr.2462

Estrany, J., Ruiz, M., Calsamiglia, A., Carriquí, M., García-Comendador, J., Nadal, M., … Gago, J. (2019). Sediment connectivity linked to vegetation using UAVs: High-resolution imagery for ecosystem management. *Science of the Total Environment*, 671, 1192–1205. https://doi.org/10.1016/j.scitotenv.2019.03.399

Fernández, C., Fernández-Alonso, J. M., & Vega, J. A. (2020). Exploring the effect of hydrological connectivity and soil burn severity on sediment yield after wildfire and mulching. *Land Degradation & Development*, 31(3), 1611–1621. https://doi.org/10.1002/ldr.3539

Fernández, C., & Vega, J. A. (2016a). Evaluation of RUSLE and PESERA models for predicting soil erosion losses in the first year after wildfire in NW Spain. *Geoderma*, 273, 64–72. https://doi.org/10.1016/j.geoderma.2016.03.016

Fernández, C., & Vega, J. A. (2016b). Modelling the effect of soil burn severity on soil erosion at hillslope scale in the first year following wildfire in NW Spain. *Earth Surface Processes and Landforms*, 41(7), 928–935. https://doi.org/10.1002/esp.3876

Ferreira, A. J. D., Coelho, C. O. A., Ritsema, C. J., Boulet, A. K., & Keizer, J. J. (2008). Soil and water degradation processes in burned areas: Lessons learned from a nested approach. *Catena*, 74(3), 273–285. https://doi.org/10.1016/j.catena.2008.05.007

Fill, J. M., Davis, C. N., & Crandall, R. M. (2019). Climate change lengthens southeastern USA lightning-ignited fire seasons. *Global Change Biology*, 25(10), 3562–3569. https://doi.org/10.1111/gcb.14727

Foerster, S., Wilczok, C., Brosinsky, A., & Segl, K. (2014). Assessment of sediment connectivity from vegetation cover and topography using remotely sensed data in a dryland catchment in the Spanish Pyrenees. *Journal of Soils and Sediments*, 14(12), 1982–2000. https://doi.org/10.1007/s11368-014-0992-3

García-Comendador, J., Fortesa, J., Calsamiglia, A., Calvo-Cases, A., & Estrany, J. (2017). Post-fire hydrological response and suspended sediment transport of a terraced Mediterranean catchment. *Earth Surface Processes and Landforms*, 42(14), 2254–2265. https://doi.org/10.1002/esp.4181

García-Comendador, J., Fortesa, J., Calsamiglia, A., Garcias, F., & Estrany, J. (2017). Source ascription in bed sediments of a Mediterranean temporary stream after the first post-fire flush. *Journal of Soils and Sediments*, 17(11), 2582–2595. https://doi.org/10.1007/s11368-017-1806-1

Gouveia, C., DaCamara, C., & Trigo, R. (2010). Post-fire vegetation recovery in Portugal based on SPOT/vegetation data. *Natural Hazards & Earth System Sciences*, 10(4), 673–684. https://doi.org/10.5194/nhess-10-673-2010

Gouveia, C., Páscoa, P., & DaCamara, C. (2018). Post-fire vegetation recovery in Iberia based on remote-sensing information. *Forest Fire*, 113–130. https://doi.org/10.5772/intechopen.72594

Heckmann, T., Cavalli, M., Cerdan, O., Foerster, S., Javaux, M., Lode, E., … Brardinoni, F. (2018). Indices of sediment connectivity: Opportunities, challenges and limitations. *Earth-Science Reviews*, 187, 77–108. https://doi.org/10.1016/j.earscirev.2018.08.004

ICNF. 2017. *Instituto Da Conservação Da Natureza E Das Florestas*. Retrieved from http://www2.icnf.pt/portal/florestas/dfci/inc/cartografia/cartografia-risco-classes-perigosidade.

Inbar, M., Tamir, M. i., & Wittenberg, L. (1998). Runoff and erosion processes after a forest fire in Mount Carmel, a Mediterranean area. *Geomorphology*, 24(1), 17–33. https://doi.org/10.1016/S0169-555X(97)00098-6

Jackson, M., & Roering, J. J. (2009). Post-fire geomorphic response in steep, forested landscapes: Oregon Coast Range, USA. *Quaternary Science Reviews*, 28(11–12), 1131–1146. https://doi.org/10.1016/j.quascirev.2008.05.003

Jain, T. B., & Graham, R. T. (2007). *The relation between tree burn severity and forest structure in the rocky mountains*. Paper presented at the In: Powers, Robert F., tech. editor. Restoring Fire-Adapted Ecosystems: Proceedings of the 2005 National Silviculture Workshop. Gen. Tech. Rep. PSW-GTR-203, Albany, CA: Pacific Southwest Research Station, Forest Service, US Department of Agriculture: pp. 213–250.

Jain, T. B., Graham, R. T., & Pilliod, D. S. (2004). Tongue-tied: Confused meanings for common fire terminology can lead to fuels mismanagement. *Wildfire*. July/August: 22–26. https://www.fs.fed.us/rm/pubs_other/rmrs_2004_jain_t002.pdf

Keeley, J. E. (2009). Fire intensity, fire severity and burn severity: A brief review and suggested usage. *International Journal of Wildland Fire*, 18(1), 116–126. https://doi.org/10.1071/WF07049

Keizer, J. J., Martins, M. A. S., Prats, S. A., Faria, S. R., González-Pelayo, O., Machado, A. I., … Varela, M. E. T. (2015). Within-in flume sediment deposition in a forested catchment following wildfire and post-fire bench terracing, North-Central Portugal. *Cuadernos de Investigación Geográfica*, 41(1), 149. https://www.researchgate.net/publication/279158670_Within-in_flume_sediment_deposition_in_a_forested_catchment_following_wildfire_and_post-fire_bench_terracing_North-Central_Portugal

Kohler, M. A., & Linsley, R. K. (1951). *Predicting the runoff from storm rainfall* (Vol. 30). Weather Bureau Washington, DC: US Department of Commerce.

Kottek, M., Grieser, J., Beck, C., Rudolf, B., & Rubel, F. (2006). World map of the Köppen-Geiger climate classification updated. *Meteorologische Zeitschrift*, 15(3), 259–263. https://doi.org/10.1127/0941-2948/2006/0130

Lanorte, A., Cillis, G., Calamita, G., Nolè, G., Pilogallo, A., Tucci, B., & De Santis, F. (2019). Integrated approach of RUSLE, GIS and ESA SENTINEL-2 satellite data for post-fire soil erosion assessment in Basilicata region (Southern Italy). *Geomatics, Natural Hazards and Risk*, 10(1), 1563–1595. https://doi.org/10.1080/19475705.2019.1578271

Larsen, I. J., & MacDonald, L. H. (2007). Predicting postfire sediment yields at the hillslope scale: Testing RUSLE and disturbed WEPP. *Water Resources Research*, 43(11), 1–18. https://doi.org/10.1029/2006wr005560

Liu, Y., Stanturf, J., & Goodrick, S. (2010). Trends in global wildfire potential in a changing climate. *Forest Ecology and Management*, 259(4), 685–697. https://doi.org/10.1016/j.foreco.2009.09.002

Martínez-Murillo, J. F., & López-Vicente, M. (2018). Effect of salvage logging and check dams on simulated hydrological connectivity in a burned area. *Land Degradation & Development*, 29(3), 701–712. https://doi.org/10.1002/ldr.2735

Mataix-Solera, J., Cerdà, A., Arcenegui, V., Jordán, A., & Zavala, L. M. (2011). Fire effects on soil aggregation: A review. *Earth-Science Reviews*, 109(1–2), 44–60. https://doi.org/10.1016/j.earscirev.2011.08.002

Mataix-Solera, J., Gómez, I., Navarro-Pedreño, J., Guerrero, C., & Moral, R. (2002). Soil organic matter and aggregates affected by wildfire in a *Pinus halepensis* forest in a Mediterranean environment. *International Journal of Wildland Fire*, 11(2), 107–114. https://doi.org/10.1071/WF02020

Mayor, A. G., Bautista, S., Llovet, J., & Bellot, J. (2007). Post-fire hydrological and erosional responses of a Mediterranean landscpe: Seven years of catchment-scale dynamics. *Catena*, 71(1), 68–75. https://doi.org/10.1016/j.catena.2006.10.006

Moody, J. A., Ebel, B. A., Nyman, P., Martin, D. A., Stoof, C., & McKinley, R. (2016). Relations between soil hydraulic properties and burn severity. *International Journal of Wildland Fire*, 25(3), 279–293.

Moody, J. A., & Martin, D. A. (2009). Synthesis of sediment yields after wildland fire in different rainfall regimes in the Western United States. *International Journal of Wildland Fire*, 18(1), 96–115. https://doi.org/10.1071/WF07162

Moody, J. A., Shakesby, R. A., Robichaud, P. R., Cannon, S. H., & Martin, D. A. (2013). Current research issues related to post-wildfire runoff and erosion processes. *Earth-Science Reviews*, 122, 10–37. https://doi.org/10.1016/j.earscirev.2013.03.004

Nunes, J. P., Naranjo Quintanilla, P., Santos, J. M., Serpa, D., Carvalho-Santos, C., Rocha, J., … Keesstra, S. D. (2018). Afforestation, subsequent forest fires and provision of hydrological services: A model-based analysis for a Mediterranean mountainous catchment. *Land Degradation & Development*, 29(3), 776–788. https://doi.org/10.1002/ldr.2776

Nunes, L., Álvarez-González, J., Alberdi, I., Silva, V., Rocha, M., & Rego, F. C. (2019). Analysis of the occurrence of wildfires in the Iberian Peninsula based on harmonised data from National Forest Inventories. *Annals of Forest Science*, 76(1), 1–17. https://doi.org/10.1007/s13595-019-0811-5

Nyman, P., Sheridan, G. J., Smith, H. G., & Lane, P. N. J. (2011). Evidence of debris flow occurrence after wildfire in upland catchments of South-East Australia. *Geomorphology*, 125(3), 383–401. https://doi.org/10.1016/j.geomorph.2010.10.016

Owens, P. N., Blake, W. H., Giles, T. R., & Williams, N. D. (2012). Determining the effects of wildfire on sediment sources using 137cs and unsupported 210pb: The role of landscape disturbances and driving forces. *Journal of Soils and Sediments*, 12(6), 982–994. https://doi.org/10.1007/s11368-012-0497-x

Prosser, I. P., & Williams, L. (1998). The effect of wildfire on runoff and erosion in native eucalyptus Forest. *Hydrological Processes*, 12(2), 251–265. https://doi.org/10.1002/(sici)1099-1085(199802)12:2<251::Aid-hyp574>3.0.Co;2-4

Robinne, F. N., Bladon, K. D., Miller, C., Parisien, M. A., Mathieu, J., & Flannigan, M. D. (2018). A spatial evaluation of global wildfire-water risks to human and natural systems. *Science of the Total Environment*,

610-611, 1193–1206. https://doi.org/10.1016/j.scitotenv.2017.08.112

San-Miguel-Ayanz, J., Schulte, E., Schmuck, G., Camia, A., Strobl, P., Liberta, G., … Kempeneers, P. (2012). Comprehensive monitoring of wildfires in Europe: The European Forest Fire Information System (EFFIS). In *Approaches to managing disaster-assessing hazards, emergencies and disaster impacts*. European Commission, Joint Research Centre, Italy: IntechOpen.

Shakesby, R. A. (2011). Post-wildfire soil erosion in the Mediterranean: Review and future research directions. *Earth-Science Reviews*, *105*(3–4), 71–100. https://doi.org/10.1016/j.earscirev.2011.01.001

Shakesby, R. A., & Doerr, S. H. (2006). Wildfire as a hydrological and geomorphological agent. *Earth-Science Reviews*, *74*(3–4), 269–307. https://doi.org/10.1016/j.earscirev.2005.10.006

Smith, H. G., Sheridan, G. J., Lane, P. N. J., Nyman, P., & Haydon, S. (2011). Wildfire effects on water quality in forest catchments: A review with implications for water supply. *Journal of Hydrology*, *396*(1–2), 170–192. https://doi.org/10.1016/j.jhydrol.2010.10.043

Smith, H. G., Sheridan, G. J., Nyman, P., Child, D. P., Lane, P. N. J., Hotchkis, M. A. C., & Jacobsen, G. E. (2012). Quantifying sources of fine sediment supplied to post-fire debris flows using fallout radionuclide tracers. *Geomorphology*, *139-140*, 403–415. https://doi.org/10.1016/j.geomorph.2011.11.005

SNIRH. (2019). *Sistema Nacional de Informação de Recursos Hídricos*. Retrieved from https://snirh.apambiente.pt/.

Stoof, C. R., Vervoort, R. W., Iwema, J., van den Elsen, E., Ferreira, A. J. D., & Ritsema, C. J. (2012). Hydrological response of a small catchment burned by experimental fire. *Hydrology and Earth System Sciences*, *16*(2), 267–285. https://doi.org/10.5194/hess-16-267-2012

Turco, M., Rosa-Canovas, J. J., Bedia, J., Jerez, S., Montavez, J. P., Llasat, M. C., & Provenzale, A. (2018). Exacerbated fires in Mediterranean Europe due to anthropogenic warming projected with non-stationary climate-fire models. *Nature Communications*, *9*(1), 3821. https://doi.org/10.1038/s41467-018-06358-z

UNOOSA. (2019). *Normalized burn ratio (NBR)*. Retrieved from http://www.un-spider.org/advisory-support/recommended-practices/recommended-practice-burn-severity/in-detail/normalized-burn-ratio.

Van Eck, C. M., Nunes, J. P., Vieira, D. C. S., Keesstra, S., & Keizer, J. J. (2016). Physically-based modelling of the post-fire runoff response of a forest catchment in Central Portugal: Using field versus remote sensing based estimates of vegetation recovery. *Land Degradation & Development*, *27*(5), 1535–1544. https://doi.org/10.1002/ldr.2507

Vieira, D. C. S., Fernández, C., Vega, J. A., & Keizer, J. J. (2015). Does soil burn severity affect the post-fire runoff and Interrill erosion response? A review based on meta-analysis of field rainfall simulation data. *Journal of Hydrology*, *523*, 452–464. https://doi.org/10.1016/j.jhydrol.2015.01.071

Vieira, D. C. S., Prats, S. A., Nunes, J. P., Shakesby, R. A., Coelho, C. O. A., & Keizer, J. J. (2014). Modelling runoff and erosion, and their mitigation, in burned Portuguese forest using the revised Morgan–Morgan–Finney model. *Forest Ecology and Management*, *314*, 150–165. https://doi.org/10.1016/j.foreco.2013.12.006

Wohl, E., Brierley, G., Cadol, D., Coulthard, T. J., Covino, T., Fryirs, K. A., … Sklar, L. S. (2019). Connectivity as an emergent property of geomorphic systems. *Earth Surface Processes and Landforms*, *44*(1), 4–26. https://doi.org/10.1002/esp.4434

Zavala, L. M. M., de Celis Silvia, R., & López, A. J. (2014). How wildfires affect soil properties. A brief review. *Cuadernos de investigación geográfica/Geographical Research Letters*, *40*, 311–331. https://doi.org/10.18172/cig.2522